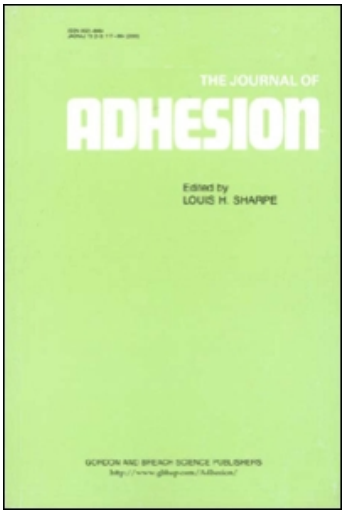

The Journal of Adhesion
Publication details, including instructions for authors and subscription information:
http://www.informaworld.com/smpp/title~content=t713453635

MOLECULAR MECHANISMS OF CELL ADHESION: NEW PERSPECTIVES FROM SURFACE FORCE MEASUREMENTS

Deborah Leckband[a]
[a] Department of Chemical and Biomolecular Engineering and Department of Chemistry, Center for Biophysics and Computational Biology, University of Illinois at Urbana-Champaign, Urbana, Illinois, USA

Online publication date: 10 August 2010

To cite this Article Leckband, Deborah(2004) 'MOLECULAR MECHANISMS OF CELL ADHESION: NEW PERSPECTIVES FROM SURFACE FORCE MEASUREMENTS', The Journal of Adhesion, 80: 5, 409 — 432
To link to this Article: DOI: 10.1080/00218460490465713
URL: http://dx.doi.org/10.1080/00218460490465713

The Journal of Adhesion, 80: 409–432, 2004

ISSN: 0021-8464 print/1545-5823 online
DOI: 10.1080/00218460490465713

Taylor & Francis
Taylor & Francis Group

MOLECULAR MECHANISMS OF CELL ADHESION: NEW PERSPECTIVES FROM SURFACE FORCE MEASUREMENTS

Deborah Leckband
Department of Chemical and Biomolecular Engineering and Department of Chemistry, Center for Biophysics and Computational Biology, University of Illinois at Urbana-Champaign, Urbana, Illinois, USA

This review highlights recent surface force measurements of the molecular interactions of protein adhesives. These studies identified novel molecular-binding mechanisms that are intimately linked to the protein structures. Central to these findings is the precise force and distance sensitivity achieved with the surface force apparatus. They illustrate that a mechanistic understanding of the nanomechanical properties of biomolecular adhesives requires measurements of both the strength of adhesion and the range of the protein interactions.

Keywords: Cell adhesion; Surface force apparatus; Cadherin; NCAM; CD2; Polysialic acid

INTRODUCTION

Cell adhesion to surfaces or to other cells is central to a multitude of processes including, for example, biofouling, viral and bacterial infection, wound healing, and embryonic development. Moreover, biological adhesives display a rich variety of properties, switching on or off in response to changes in pH or metal concentrations [1], for example. Other bonds strengthen or weaken in response to applied force [2, 3].

Received 16 December 2003; in final form 25 March 2004.

One of a collection of papers honoring Jacob Israelachvili, the recipient in February 2003 of *The Adhesion Society Award for Excellence in Adhesion Science, Sponsored by 3M*.

This work was supported by NIH 1 RO1 GM63536 and by NIH 2 RO1 GM551338.

Address correspondence to Deborah Leckband, Department of Chemical and Biomedical Engineering, University of Illinois at Urbana-Champaign, 600 S. Mathews Avenue, Urbana, IL 61801, USA. E-mail: leckband@uiuc.edu

Cell adhesion has both commercial importance and fundamental biological significance. The ability to control or exploit the biological components responsible for this behavior hinges on the elucidation of the fundamental molecular design rules governing their adhesive function.

To first order, colloidal forces govern cell interactions. Absent specific adhesive proteins on their surfaces, cells would generally repel due to the substantial repulsive colloidal forces between them [4–6], arising from negatively charged lipids, proteins, and both charged and neutral carbohydrates. While there is a weak van der Waals attraction between the membranes, the net intercellular forces are primarily repulsive (Figure 1). The dense carbohydrate surface coating (glycocalyx) in particular can extend several hundred Ångstroms from the membrane, and is the principal repulsive barrier at the cell surface. Thus, cells adhere to other cells or substrates *via* specific molecular binders displayed on their surfaces. These adhesive proteins generate sufficient attractive forces to overcome or circumvent the large, repulsive barriers. Alternatively, they could generate adhesive interactions at distances beyond the range of the repulsive terms.

In order to form the types of tight, protein-mediated junctions seen between cells, the steric barriers would have to be compressed or displaced from the contact zone. Alternatively, as in the case of yeast or fungi, adhesins may be covalently linked to the outer edge of the dense carbohydrate barrier [7]. In higher, multicellular organisms, the adhesion receptors are anchored to the lipid membranes and either displace the barriers [8] or engage their complementary receptors at distances beyond the range of repulsion (Figure 1) [9–11]. The latter suggests that both the tensile strengths of the bonds and the intersurface binding distance control cell adhesion.

A distinctive feature of many adhesion proteins is their molecular architecture. The structures of most cell adhesion proteins comprise single polypeptide chains that fold into multiple, tandemly repeated domains [10, 11]. Figure 2 shows cartoons of the multidomain structures of some common adhesion proteins. These cartoons are based on biochemical data, some structural data, and sequence homologies with proteins of known structure [10]. Proteins related to those shown are not rigid rods, in most cases, but their structures are much stiffer than unstructured polymer chains. The individual modules differ in their chemical composition while possessing very similar overall structures. The atomic level structures of only a few of these proteins have been determined, due to the difficulty in crystallizing such large macromolecules. In some instances, the structures of protein fragments were determined, and in some cases the exact binding inter-

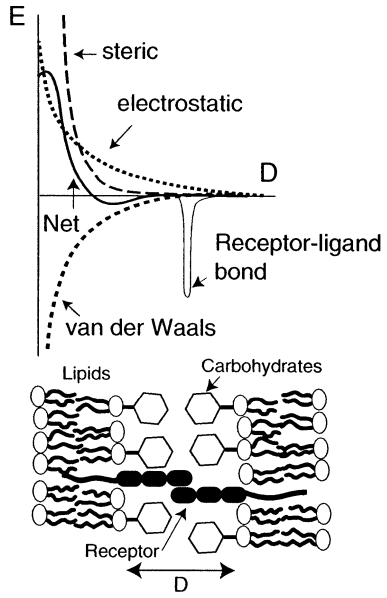

FIGURE 1 Hypothetical interaction potential between cell membranes.

faces have been elucidated [10]. The domain lengths are ~ 4 nm, so that the total end-to-end lengths of the protein segments on the exterior cell surface (extracellular domains) can be several hundred Ångstroms. The proteins in Figure 2 are a very small subset of the now hundreds of known cell adhesion molecules (CAMs) [10, 11].

One hypothesis for the functional significance of this molecular design is that the modular architectures could enable the proteins to bridge cell membranes at relatively large distances [9]. However, this hypothesis can only be tested by comparing the range and magnitude of the receptor-ligand (binding partner) attraction relative to the repulsive forces between cells. To this end, my laboratory is conducting surface force measurements of the force-distance profiles of several different adhesion proteins [12–15]. These studies uncovered much richer mechanisms than the simple picture suggested by Figure 1. Other force probe techniques such as atomic force microscopy and optical tweezers have been used to determine the strengths of protein bonds [16] or the force-induced unfolding of proteins [17]. However, as demonstrated in this review, these techniques lack the absolute distance resolution [18] required to determine how protein structures and their binding modes impact intersurface potentials.

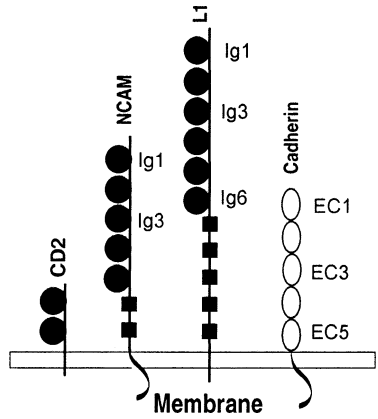

FIGURE 2 Multidomain structures of representative cell adhesion proteins. These cartoons illustrate schematically the structures of adhesion proteins CD2, NCAM, L1, and cadherin. The filled circles represent "immunoglobulin-type" (Ig) structural modules or domains, the squares are "fibronectin type III" (FN III) structural domains, and the open ovals are "cadherin" (EC) domains. The proteins are anchored to the membranes by lipids or protein segments, some of which extend inside the cell. These architectures are inferred primarily on the basis of biochemical data, sequence analysis, and homology with other related proteins [10, 11].

This review describes our recent surface force measurements of adhesion proteins that have elucidated molecular design rules underlying the function of some of these important proteins. The measurements focus on the relationships between the modular protein architectures (*c.f.* Figure 2) and their impact on intersurface potentials, their molecular mechanisms of binding and adhesive failure, and their regulation by posttranslational modifications. These findings exemplify the centrality of both the magnitudes and the ranges of molecular interactions in bioadhesion. They also illustrate the power of surface force measurements to both quantify these parameters and determine molecular mechanisms of bioadhesion.

SURFACE FORCE MEASUREMENTS REVEAL NOVEL MECHANISMS OF BIOLOGICAL ADHESION

Surface Force Apparatus

The surface force apparatus (SFA) technique is used to quantify the ranges and magnitudes of the forces exerted between two extended

surfaces as a function of their separation distance [19]. In these experiments, sample materials are coated on the surfaces of cleaved mica sheets that are glued to the surfaces of two curved macroscopic fused silica lenses. The back surfaces of the mica are coated with a reflective silver film, so that the region between the silver mirrors is the resonant cavity of a Fabry-Perot interferometer [20]. White light incident on the interferometer generates a series of interference fringes of equal chromatic order (FECO), whose wavelengths are determined by the thickness and refractive index of the various films between the two silver mirrors. From the wavelengths of these fringes, we determine the absolute surface separation with a resolution of ± 1 Å [20].

The total force between the surfaces is determined with a resolution of ± 0.1 mN/m from the deflection of a sensitive leaf spring that supports the lower disk [19]. The silica disks are machined to the shape of hemicylinders, and the opposite disks are oriented at right angles to each other so that they contact at a point. Because the net force between the disks scales with the surface dimensions, the total measured force between the curved surfaces, F_c, is normalized by the geometric average radius of the hemicylinders, $R = (R_1R_2)^{1/2}$: F_c/R [21]. The sensitivity in the normalized force, F_c/R, between these extended surfaces is sufficient to measure weak forces such as the van der Waals attraction between membranes [22]. This instrument is currently the most sensitive technique for quantifying the normalized force-distance profiles between surfaces over large distances [18].

The normalized force, $F_c(D)/R$, between the hemicylinders is related to the corresponding interaction energy per unit area, $E_f(D)$, between two equivalent planar surfaces by the Derjaguin Approximation: $E_f = F_c/2\pi R$ [23]. This relationship holds when the separation distance $D \ll R$. The Derjaguin approximation thereby directly relates the total integrated force measured with the SFA to the interaction potential between extended planar surfaces of identical composition. The geometry only affects the measurements through the $2\pi R$ scaling prefactor. Additionally, the adhesion energy per area, E_{ad}, between the two surfaces is determined from the normalized pulloff force, F_{po}/R. According to the Johnson-Kendall-Roberts theory [18, 24], these quantities are related by $E_{ad} = 2F_{po}/3\pi R$. The adhesion energy per bond can be estimated by normalizing the adhesion energy by the protein coverage Γ. The estimated energy per bond is thus E_{ad}/Γ. This scaling, however, assumes that all proteins on the surfaces engage in adhesion, and that all proteins in the population are active. In addition, on fluid membrane surfaces some proteins may be convected to the perimeter of the contact region, increasing the protein

density at the edge [25]. Thus, the energy per bond determined from JKR theory and the protein density is merely an estimate, and is generally accurate to within a factor of 2–3 of the bond energies determined from equilibrium-binding measurements [26, 27].

In summary, the SFA measurements directly quantify the intersurface potentials and the adhesion energies between surfaces, both of which are central parameters defining cell adhesion [9].

Dual Functions: Cell Adhesion Proteins as Scaffolds and Adhesives

Cellular-based immunity results from interactions between thymus cells (T cells) and antigen-presenting cells (APCs). Several proteins mediate this intercellular association, and the adhesive junction that forms between the cells is referred to as the "immunological synapse" [28, 29]. This association triggers an immune response. In particular, binding between two principal proteins called the major histocompatibility complex on the APC and the T cell receptor (TCR) on T cells triggers the response [30]. However, both the formation of the "immunological synapse" and the association of the MHC and TCR are facilitated by a host of auxiliary proteins. The latter proteins display a range of dimensions and kinetic properties that are believed to drive their organization into functionally significant protein patterns at the cell–cell junctions [29, 31].

One pair of these auxiliary proteins is CD2 on T cells and its ligand CD48 (in rats) on APCs [32–34]. The structures of the individual proteins have been determined [35–38], but their complex has not been crystallized. CD2 and CD48 comprise two tandemly linked structural modules—immunoglobulin (Ig) type domains—that are bound to cell membranes by hydrophobic anchors (Figure 2). The ligands of CD2 all have similar structures to CD2, although their chemical compositions differ substantially [32, 33]. The linear dimensions of the extracellular regions of CD2 and its ligands are ~ 75 Å (Figure 3) [33].

Biochemical evidence suggests that CD2 binds its ligands in a head-to-head orientation such that the complex spans a membrane gap of $\sim$135Å (Figure 3a) [33]. The complex formed between the outer domains of human CD2 and CD58, which is the human homolog of CD48 [39], suggests that the adhesive interface is stabilized by several ionic bonds between charged amino acids on the opposing proteins [40]. Moreover, the ~ 135 Å membrane gap spanned by the complex is thought to be important because models of the complex match the dimensions of the MHC-TCR complex. Thus, CD2 has been proposed

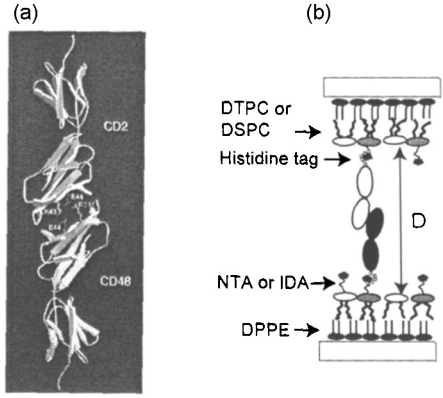

FIGURE 3 (a) Proposed model of the CD2-CD48 complex (from Davis and van der Merwe [33]). (b) Illustration of the oriented protein arrays used in surface force measurements. The proteins were engineered with hexahistidine polypeptide tags at their C-terminal ends. These tags bind directly to the NTA headgroups in the outer leaflet of the supported lipid bilayers. The proteins self-assemble on the reactive membranes to form oriented monolayers. Modified from Davis and van der Merwe [33].

to act as a scaffold, which controls the intermembrane spacing, enabling the correct alignment of MHC and TCR between adjacent cells [32, 33].

To test this structural binding model and to quantify the adhesion energy of the rCD2-CD48 bond, Zhu *et al.* used the surface force apparatus to measure the normalized force *versus* distance profiles between protein-coated membranes [12]. rCD2 and CD48 are among the most studied proteins in this class. In the force measurements, a model cell membrane was constructed by selectively binding the proteins to the surfaces of lipid bilayers, supported on mica sheets. These are fixed to the surfaces of transparent silica lenses in the apparatus (Figure 3b). The proteins were engineered with short polypeptide tails (hexahistidine) on their C-terminal ends to ensure their selective immobilization and proper orientation on the membranes. This short hexahistidine tether specifically anchors noncovalently to the nitrilotriacetic acid (NTA) headgroups of synthetic lipids in the supporting membranes, so that the proteins bind to the membranes and orient as shown in Figure 3b. Thus, the integrated force measured between the two hemicylindrical disks represents a uniform, homogeneous protein population.

Figure 4 shows the normalized force-distance profiles measured between the oriented arrays of CD2 and CD48. The distance, D, is the

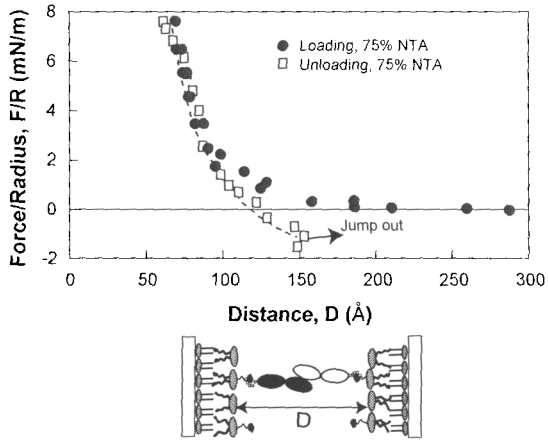

FIGURE 4 Normalized force *versus* distance profiles measured between CD2 and CD48. Forces were measured between the oriented CD2 and CD48 monolayers as a function of the distance D between the bilayers. The proteins repel at $D < 160\,Å$ but adhere during separation. The out arrows indicate the point of adhesive failure between the protein monolayers. Modified from reference 12.

distance between the surfaces of the lipid membranes (*c.f.* Figure 3b). In these measurements, the forces are measured during both approach (loading) and separation (unloading). During approach the onset of the repulsion at $D < 160\,Å$ agrees with the expected range of steric repulsion between end-on oriented proteins. Separation of the membranes resulted in the hysteresis due to the protein–protein attraction. Adhesive failure occurred at a membrane distance of $153 \pm 5\,Å$ [12], which is the position of the maximum gradient in the intersurface potential. The latter distance includes a $\sim 10\,Å$ contribution from each of the anchoring tethers. Thus, the complex dimensions are $153 \pm 5 - (2 \times 10\,Å) = 133 \pm 5\,Å$, which agrees quantitatively with the predicted molecular dimensions of the complex [33].

The adhesion energy measured with these proteins was relatively low. From the pulloff force of $-1.3 \pm 0.2\,mN/m$, the adhesion energy density is $\sim 0.3\,mJ/m^2$ [12]. At $D = 153\,Å$, this is too small to be due to the van der Waals attraction between the bilayers, which is estimated to be $\sim 4 \times 10^{-3}\,mN/m$ at this distance. The adhesion is thus attributed to protein binding [22]. Normalizing the energy density by the protein coverage on the membranes ($6.6 \pm 0.3 \times 10^4/\mu m^2$), the estimated energy per bond is $1.2 k_B T$, where k_B is the Boltzmann constant and T is the absolute temperature. Because these bonds

are relatively weak, cell–cell junctions likely involve many proteins in order to stabilize the junctions and elicit a biological response [28, 29]. The absolute density needed for this is unknown, however, because the latter is more a functional definition–that is, what stimulates the correct biological response—than a quantitative one.

The absolute distance-measuring capability of the SFA thus enabled the direct verification of the predicted CD2-CD48 complex dimensions. These surface force measurements were also the first to confirm directly that the CD2-CD48 complex is structurally matched to the dimensions of the TCR-MHC complex, which the adhesive junctions must accommodate. The membrane separation spanned by the complex also supports the proposed scaffolding role of these adhesion proteins.

Modular Architectures Allow Adhesive Junction Assembly in Multiple, Sequential Steps

A second class of adhesion proteins, cadherins, forms tight intercellular junctions in soft tissues by binding to identical proteins on adjacent cells [1]. In addition to maintaining the structural integrity of soft tissues, the proteins also play an important role in tissue morphogenesis [41, 42]. At an early stage an embryogenesis, cells begin to sort out into three cell layers by a process called gastrulation [30]. These three germ layers in turn differentiate, roughly, into the different organ systems of the organism. This cell segregation process depends on the different cadherins expressed on the cells comprising these different layers.

Classical cadherins consist of an adhesive, extracellular region, a membrane-spanning segment, and an intracellular domain (Figure 2). The polypeptide segment on the outer surface of the cell folds into five tandemly arranged extracellular (EC) domains that are each 43 Å in length and are numbered 1–5, beginning at the outermost domain (Figure 2) [1]. The structural folds of the EC domains are similar, but their compositions differ. There are five different classical cadherins: namely, epithelial (E-), neural (N-), compaction (C-), placental (P-), and cardiac (R-) cadherins. These are each classified according to their tissue specificity, and they display different binding selectivity. For example, N-cadherin is located primarily in nerve tissue, and it adheres to N-cadherin but not to E-cadherin, which is expressed in epithelial tissue [41].

There are two main hypotheses for the molecular basis of cell segregation during gastrulation. The "differential adhesion hypothesis" postulates that differences in cohesion between identical cadherins,

e.g., N-Cad/N-Cad *versus* adhesion between different cadherins, *e.g.*, N-Cad/E-Cad, drives cell segregation by the same physics that govern liquid–liquid phase separation [43, 44]. On the other hand, the "chemoaffinity hypothesis" postulates that cell segregation is driven by selective molecular recognition events, which in turn trigger processes that drive the cell segregation [45]. These mechanisms are not mutually exclusive and they do share some features, but they have not yet been tested at the molecular level.

An initial model for cadherin adhesion proposed that the proteins bind at large (385–400 Å) cell–cell distances through their end (EC1) domains [46]. The crystal structure of the cadherin ectodomain suggests the proteins adhere merely by inserting the hydrophobic side chain of a tryptophan amino acid in EC1 into a hydrophobic pocket of the EC1 domain of an opposing protein. Early studies localized the tissue specificity to this domain [47], and the mutation of the tryptophan in the EC1 domain appeared to abrogate adhesion [48]. However, this binding interaction is highly conserved in all classical cadherins, which begs the question of the molecular basis of cadherin selectivity. On the other hand, other experimental data suggest a more complex mechanism that involves additional cadherin domains. Studies with cadherin fragments showed that strong cell adhesion requires more than the EC1 domain alone [49]. Another study showed that cells still adhere weakly after removing the EC1 domain [50].

Direct force measurements of cadherin adhesion revealed a more complex mechanism that involves the formation of multiple bound states with different strengths [13–15]. Surface force measurements were used to test the initial model based on crystallography by directly quantifying the distance dependence of the forces between oriented monolayers of cadherin extracellular domains [13–15]. Genetically engineered fragments of the cadherin were bound and oriented on planar lipid bilayers as described above for CD2 and CD48. X-ray reflectivity studies further confirmed that the proteins are oriented normal to the membrane surface, as shown in Figure 5 (lower panel) [51].

Instead of forming a unique complex at a single intermembrane distance, the normalized force-distance measurements showed that cadherin forms three bound states, each of which spans a different membrane separation (Figure 5). In particular, the cadherins bound at 250 ± 10 Å, 330 ± 10 Å, and 400 ± 10 Å (Figure 5, lower panel) [14, 15]. The positions of these three adhesive states correspond to the relative domain alignments shown in Figure 5. The strongest adhesion involves the full interdigitation of the antiparallel proteins. The weakest bond is between the outermost domains (EC1).

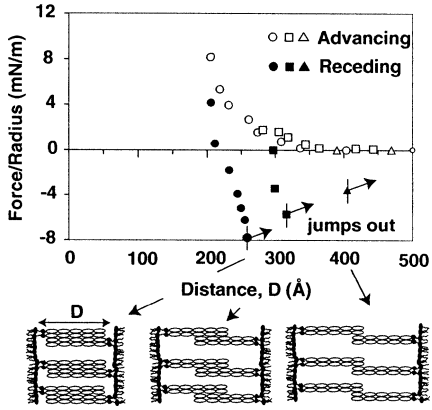

FIGURE 5 Normalized force *versus* distance between cadherin extracellular domains. The force–distance profiles were measured between oriented cadherin monolayers. During approach, the proteins repel at D < ~400 Å. Upon separation from distances between 250 Å and 400 Å, the proteins adhere at the three different membrane separations indicated by the out arrows at the minima in the curves. The three bound states correspond with the three relative protein alignments shown in the cartoon. Modified from Sivasankar *et al.* [14].

Independent atomic force microscope (AFM) studies of cadherin binding also detected three bound states [52]. However, because of the inability to measure the absolute separation distance with the AFM, the latter authors were unable to determine the structural origins of their observations.

This multisite cadherin-binding mechanism illustrated in Figure 5 was initially based on a geometric interpretation of the normalized force–distance profiles. Both the model and the identities of the adhesive domains are now supported by force measurements with genetically engineered cadherin fragments [13]. By engineering cadherin extracellular regions that lacked different EC domains [49] we determined how distinct domains contribute to the oscillatory force–distance profile in Figure 5 (upper panel). By selectively deleting domains EC12, EC3, EC4, and EC5, we confirmed that EC3/EC3 EC3 contacts form the strongest, bound state at 250 Å [13]. Direct EC1/EC1 contacts form the outer, weakest bound state, and the intermediate state requires EC1 and EC3 [13]. Removing EC5, for example, reduced the protein length by 43 ± 2 Å [53]. The EC1–4 fragments nevertheless displayed three bound states, but the positions of their adhesive minima were shifted in by 86 Å ($=2 \times 43$ Å) (Table 1). Removing EC4 and EC5 shifted the three bound states inward by an

additional 86 Å, in quantitative agreement with the change in the protein lengths (Table 1). Thus, EC4 and EC5 do not contribute significantly to homophilic cadherin adhesion. By contrast, removing EC3 alone (EC1245) eliminated the inner and intermediate bonds, but the proteins still bound through their outer domains. Likewise, removing EC12 abolished the middle and outer bonds, but EC345 fragments bound at a distance that agreed quantitatively with contact between EC3 domains (Table 1). Six different engineered proteins were used, and measurements were conducted both between identical proteins and between different protein fragments [13]. The aggregate data in Table 1 established the domain interaction model in Figure 5 (lower panel).

These force measurements are supported by independent cell adhesion studies with these deletion mutants [49] and by cell aggregation studies with similar truncated cadherin fragments [50]. This modular cadherin architecture therefore appears to generate a modular binding mechanism that involves multiple segments of the molecule. This unusual mechanism contrasts with most recognition interactions, which typically involve unique binding sites on both the receptor and ligand, *e.g.*, CD2 and CD48.

Although the binding interface between the outer EC1 domains was identified in crystal structures of both the full-length extracellular region and the outer two EC1 and EC12 domains [46, 54, 55], the binding interface of the EC3/EC3 contact and the middle bound state have not yet been established. The absence of these structural data is due to the fact that only one structure of the full-length cadherin has been solved, and there was only one adhesive interface reported in that structure [53]. However, the bound states identified by force measurements are mutually exclusive. It is highly unlikely that the crystal lattice would accommodate all three contacts. More work is clearly required to define the structures of the other interfaces. In this instance, the absence of the additional adhesive interfaces in the crystal means only that those interfaces were not compatible with the lattice formed under the crystallization conditions used. Although the surface force measurements don't identify the exact binding interface, they can identify the functional regions in the absence of structural data, and they allow the direct testing of different models.

If a single bound state is sufficient to bridge two cells, what could be the significance of having multiple binding sites? The direct force measurements revealed a possible consequence of this hierarchy of bound states. Ordinarily, once the receptor-ligand bonds break under force, the surfaces snap apart (< 1s) from the position of the maximum gradient in the intermolecular potential [18]. In contrast to the latter

TABLE 1 Adhesion Between Cadherin Ectodomain Fragments

Cadherin fragment	1st minimum (inner)	F/R, mN/m	2nd minimum (middle)	F/R, mN/m (energy per bond, kT)[a]	3rd minimum (outer)	F/R, mN/m
CEC1-5 vs. CEC1-5	384 ± 6 Å	−3.6 ± 0.4	445 ± 10 Å	−2.4 ± 0.5	531 ± 6 Å	−1.8 ± 0.6
CEC1-4 vs. CEC1-4	297 ± 6 Å	−1.4 ± 0.3	356 ± 2 Å	−0.9 ± 0.2	431 ± 2 Å	−0.22 ± 0.02
CEC1-3 vs. CEC1-3	211 ± 9 Å	−1.2 ± 0.3	269 ± 2 Å	−0.15 ± 0.01	349 ± 5 Å	−0.17 ± 0.05
CEC1-2 vs. CEC1-2	—	—	—	—	271 ± 14 Å	−0.3 ± 0.1
CEC3-5 vs. CEC3-5	386 ± 4 Å	−0.5 ± 0.1	—		—	
CEC1245 vs. CEC1245	—		—		424 ± 8 Å	−0.7 ± 0.1
CEC123 vs. CEC345	285 ± 9 Å	−0.5 ± 0.2	—		—	
CEC1245 vs. CEC345	—		—		—	
CEC1-5 vs. CEC1245	—		—		493 ± 6 Å	−1.3 ± 0.2
CEC1-5 vs. CEC345	375 ± 8 Å	−0.9 ± 0.2	—		—	

The adhesion was measured between different cadherin fragments. Both of the positions of the adhesive bonds and the magnitude of the adhesion are indicated.

behavior, upon rupture of the deeply bound state (250 Å) the cadherin layers instead separated slowly over a distance of ~200 Å, which is the length of the extracellular domain [14]. This separation rate was directly quantified, at the molecular level, from the time-dependent changes in the interference fringes used to measure distances in the surface force apparatus [14]. The spontaneous detachment occurred in three stages, marked by different separation velocities (Figure 6). The transitions between the three velocity regimes occurred roughly at the locations of the three attractive minima (Figure 6) [14]. Thus, upon failure of the strongest bond (250 Å), the protein detachment appears to be slowed by additional binding at the middle and outer minima, before finally abruptly breaking contact. The proposed explanation for this "viscous" pulloff is that the sequential rupture and formation of multiple bonds along the unbinding trajectory slows the kinetics of adhesive failure.

Conversely, if the proteins are brought to a distance where only their EC1 domains contact, *i.e.*, at 400 Å, then the protein monolayers spontaneously jump-in to the primary, lower energy configuration at 250 Å [14]. This process was directly observed with the interferometer of the SFA. Thus, the potential energy gradient, generated by the hierarchy of bond strengths, drives the spontaneous zipping-up of the protein–protein junction. This jump-in, which occurs when the gradient of the intersurface potential exceeds the spring constant [19], occurs slowly over a period of ~5 min. These dynamics suggest

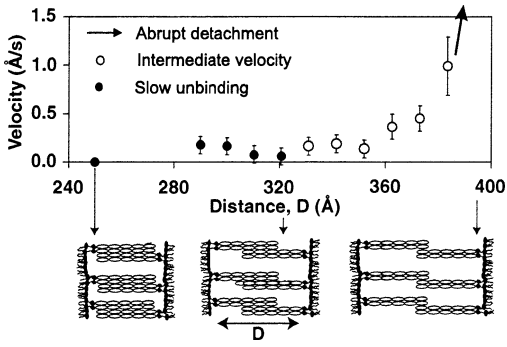

FIGURE 6 Detachment velocity *versus* distance following the failure of cadherin bonds. The rate at which the proteins jump out of contact was quantified from the time-dependent changes in the interference fringes. Once the bonds at 250 Å fail, the proteins separate slowly at ~0.1 Å/s and then begin to accelerate at D > 320 Å. They abruptly snap out of contact from ~390 Å. Modified from Sivasankar *et al.* [14].

that the outer, weak bonds may initially engage cells at large membrane separations, and enable the subsequent, slower formation of stronger bonds. Ongoing structural studies as well as kinetic measurements are now testing the impact of the different bound states on the dynamics and mechanisms of cadherin junction assembly.

Nonspecific Colloidal Forces Regulate the Neural Cell Adhesion Molecule (NCAM)

The Molecular Mechanism of NCAM Adhesion

The neural cell adhesion molecule, NCAM, also mediates cell–cell adhesion by binding to identical proteins on adjacent cell surfaces during neural development [11]. This essential protein is one of the most abundant adhesion proteins in the brain, and it is linked to long-term memory formation and circadian rhythms [11]. NCAM is also a multidomain adhesion protein, and its extracellular region contains seven modular repeats, which are structurally similar but differ in their chemical composition [10] (Figure 2). The architecture in Figure 2 is based primarily on biochemical data and sequence analyses [11]. The first five domains are immunoglobulin-type (Ig) domains and are numbered 1–5 (Ig1–5), beginning with the outermost domain. The last two domains are referred to as fibronectin type III (FN III) repeats. An additional feature of the extracellular domain is the distinct bend between the Ig5 and the first fibronectin domain identified by electron microscopy [56, 57] (Figure 2). The functional significance of the latter has not been determined.

There are three different models for the mechanism of homophilic NCAM binding (Figure 7). These models are based on binding studies with NCAM fragments, solution NMR and X-ray structures of NCAM fragments, and the ability of peptides to inhibit NCAM-mediated cell adhesion. Model 1 (Figure 7a) proposes that the NCAM adhesive complex involves the fully aligned, antiparallel Ig1–5 segments. Studies with different NCAM fragments identified Ig3 as the principal adhesive domain. The latter findings indicated that Ig3/Ig3 contacts form the strongest NCAM bond, and heterophilic binding by the flanking domains augment the adhesive strength [58]. However, removing this domain abrogated cell adhesion [59]. Despite these findings, attempts to measure the self-association of excised Ig3 domains in solution failed to detect any interaction [60, 61].

Model 2 (Figure 7b) is based on equilibrium binding studies with NCAM fragments [62], and on both X-ray and NMR structures of a complex between the outer Ig1 and Ig2 domains [62–64]. In this model, the outer Ig1 and Ig2 domains form an antiparallel complex

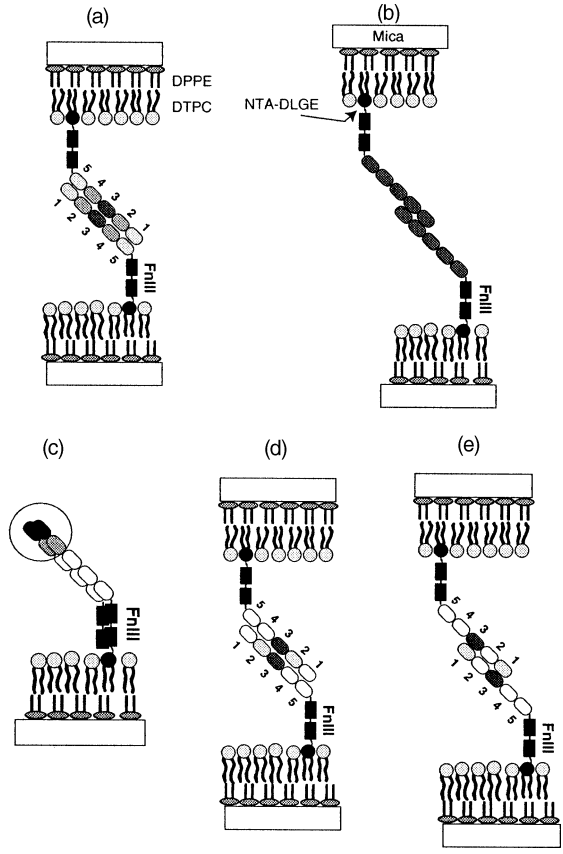

FIGURE 7 Proposed models for homophilic NCAM adhesion. (a) In Model 1, the proteins are proposed to form a complex via the antiparallel overlap of the Ig1–5 regions [58, 59]. (b) Model 2 proposes that NCAM binds via the double-reciprocal association of Ig1 and Ig2 domains [61]. (c)–(e) In Model 3, NCAM is proposed to associate laterally via the Ig1 and Ig2 domains (c). In addition, opposing proteins bind by the association of the Ig2 and Ig3 domains (d), as well as between the Ig1 and Ig3 domains [65]. Modified from Johnson *et al.* [66].

mediated by saltbridges between the two proteins. The data demonstrating the functional relevance of this interaction are nevertheless contradictory [60].

Finally, Model 3 (Figures 7c–7e) is based on the crystal structure of the Ig1–3 fragment and on the ability of certain peptides to inhibit NCAM-mediated cell adhesion [65]. In this model, the Ig1 and Ig2 domains are proposed to form bonds between proteins on the same

membrane. An additional proposed bond lies between antiparallel Ig1 and Ig3 domains, and they proposed an interface between antiparallel Ig2 and Ig3 domains [65]. This model, while accounting for some of the data used to support Models 1 and 2, predicts an entirely different binding pattern between NCAM extracellular regions (Figure 7c–7e).

Directly measured force–distance profiles between membrane-anchored NCAM extracellular domains discriminated between these different possibilities. Each model in Figure 7 predicts NCAM binding at a different membrane distance. Because of the bend in the protein, the simplest measurement to interpret is that between engineered Ig1–5 fragments bound to the membrane *via* C-terminal hexahistidine tags. The binding distances between these Ig1–5 fragments validated Models 1 and 2 and disproved Model 3.

Figure 8 (upper panel) shows the normalized force–distance profile between oriented Ig1–5 domains [66]. X-ray and neutron reflectivity studies verified the end-on orientation of the protein (unpublished results). The length of the Ig1–5 segment is also $\sim 180\,\text{Å}$ [56]. The proteins bound at two-membrane gap distances corresponding to the domain overlaps in Figure 8 (lower panel). The adhesion at $80 \pm 5\,\text{Å}$ agrees with Model 1 (Figure 7a), in which the proteins bind in a fully aligned configuration. Similarly, the second bound state at $290 \pm 5\,\text{Å}$ agrees quantitatively with Model 2 (Figure 7b), in which NCAM forms a double-reciprocal bond between Ig1 and Ig2. In contrast to Model 3, the latter finding confirms that the Ig1 and Ig2 domains bind to the Ig1 and Ig2 domains on an opposed NCAM molecule. The force data are also incompatible with the Ig1–Ig3 interface proposed by Model 3 (Figure 7e). The third interface proposed by Model 3 (Figure 7(d)) could not be ruled out from the binding distances alone, but it was eliminated by studies with different NCAM domain deletion mutants [66]. As with cadherin, additional force-distance measurements with both the full NCAM extracellular domain and with Ig domain deletion mutants confirmed the model indicated in Figure 8(lower panel). Therefore, as with cadherin, the modular structure of NCAM similarly generates a modular binding mechanism.

This example further illustrates the importance of determining both force and distance in evaluating the adhesion mechanisms of these complicated molecules. Traditional biophysical approaches such as equilibrium binding measurements and crystallography can provide important information concerning the binding mechanisms. However, measurements of force and the absolute distance give unique functional and structural information that may be difficult to deduce from individual, static structures and single parameters such as binding affinities.

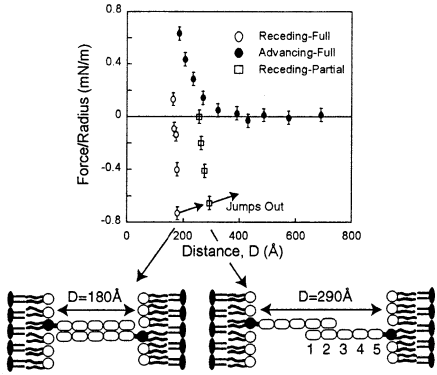

FIGURE 8 Normalized force *versus* distance profiles between membranes coated with oriented Ig1–5 fragments. The engineered Ig1–5 segment of NCAM was immobilized on supported lipid bilayers. During approach (upper panel, filled circles), the proteins repel at distances $D < 350$ Å. Upon separation (lower panel, open circles), the proteins adhere at 180 ± 10 Å and at 290 ± 10 Å. The lower panel shows the domain alignments consistent with these force data. Modified from Johnson *et al.* 66.

Regulating NCAM Adhesion by Nonspecific Colloidal Forces

Perhaps one of the most interesting features of NCAM is that it has two forms: an adhesive form and an antiadhesive form [67, 68]. The antiadhesive form is covalently modified with two long, linear polymers of polysialic acid (PSA) attached to the fifth Ig domain of the extracellular region [69]. The adhesive form is unmodified. The antiadhesive form is linked to neural plasticity in the developing brain, to the regulation of circadian rhythms, and to tumor progression in some cancers [67, 70, 71].

In vivo, cell surfaces in different tissues or at various stages in development display different amounts and types of carbohydrates. In particular, high levels of PSA in the brain are associated with neural plasticity—or the ability to break and form new cell contacts—in the early stages of development [67, 68, 72]. Electron micrographs also show that PSA modification of NCAM increases intercellular spacing [73]. In one hypothesis, PSA's biological activity is attributed to increased intersurface repulsion by the grafted polyelectrolytes that weaken intercellular adhesion (Figure 9a) [67, 68, 74]. Although such steric repulsion is not unfamiliar to colloid scientists [75], biological regulation is typically believed to occur *via* specific interactions rather than nonspecific colloidal forces. An alternative explanation, however, is that PSA disrupts interactions between

proteins on the same cell surface (Figure 9c) and thereby switches off their adhesive activity [11]. The latter mechanism requires that PSA only act within the plane of the membrane, whereas the former requires PSA to influence intermembrane forces at least to the range of homotypic NCAM binding. In other words, if PSA attenuates NCAM adhesion by nonspecific steric repulsion, then the increased repulsion should be sufficient to overwhelm both bound states of NCAM.

Surface force measurements carried out with both the modified and unmodified NCAM ectodomains directly demonstrated that PSA increases the nonspecific intermembrane repulsion at the expense of the intersurface adhesion (Figure 10) [76]. The range of the adhesive interactions between unmodified NCAM is slightly different from that in Figure 9 due to the addition of the two FNIII domains and the bend at the FN III–Ig5 junction. Although the range of the repulsion between PSA-NCAM monolayers was only slightly larger than

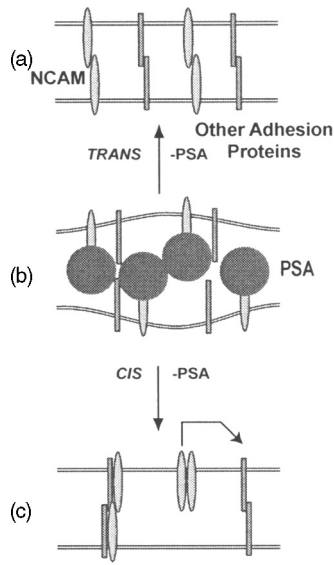

FIGURE 9 Proposed mechanism of the PSA-modulation of NCAM adhesion. (a) NCAM and other proteins bridge cell membranes by interacting with identical, monomeric proteins on the opposite membrane. PSA modification is proposed to increase the excluded volume of NCAM and hence the disjoining pressure between the membranes (b). Alternatively, protein dimers on the same membrane are proposed to bind to dimers on the opposite membranes (c). PSA modification disrupts these lateral interactions, switching off the adhesive function and causing the membranes to separate (b). Modified from Rutishauser [67].

between NCAM in 150 mM 1:1 electrolyte, the magnitude of the repulsion increased significantly. This was sufficient to abrogate adhesion at both binding distances (Figure 10) [76].

The ionic strength dependence of the repulsion due to PSA demonstrates that the abrogation of adhesion was due to nonspecific colloidal forces. PSA is a polyelectrolyte, and the hydrodynamic radius depends on the ionic strength [77]. Thus, in 1 M electrolyte, the repulsion decreased substantially as the chains collapsed. In turn, the protein attraction reemerged at the same distances as measured with unmodified protein [76]. Thus, merely tuning the electrosteric repulsion with salt modulates the impact of PSA on NCAM-mediated adhesion. Furthermore, the enzymatic cleavage of the polysialic acid chains restored the adhesion at both membrane separations [76]. These data confirm that PSA modulates cell adhesion primarily by increasing the nonspecific repulsion between membranes at the expense of the protein-mediated attraction. This mechanism contrasts dramatically with the vast majority of regulatory processes in biology that involve specific protein interactions or enzyme reactions [30].

While this is one example in which biology actively uses colloidal forces to modulate biological function, other proteins are emerging as possible candidates for this type of regulatory mechanism. For example, neurofascin is another large, multidomain adhesion protein that plays a role in axon guidance and neural development [78]. Similar to NCAM, it is also present in multiple forms, and the antiadhesive

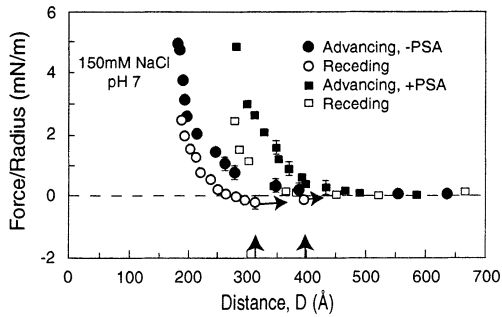

FIGURE 10 Normalized force *versus* distance profiles between NCAM and PSA-NCAM monolayers. The circles show the force–distance profile measured between unmodified, adhesive NCAM during approach (filled symbols) and retraction (open symbols). The out arrows indicate the locations of bond failure, and the upward pointing arrows show the distances where this occurs. The filled and open squares show the force–distance profiles measured during, respectively, approach and separation of PSA-NCAM monolayers. Modified from Johnson *et al.* [76].

form of neurofascin contains a region that is extensively decorated with carbohydrates [78]. It remains to be seen whether these carbohydrates have a similar impact on neurofascin-mediated cell adhesion. Importantly, as we demonstrated in these examples, clarifying the molecular basis of the modulation of the adhesive functions of these proteins requires the ability to quantify the ranges and magnitudes of both the attractive and repulsive forces controlling the adhesion between cell membranes.

SUMMARY

These examples highlight recent force measurements that have led to a better understanding of the molecular mechanisms by which cells form adhesive contacts. They clearly show the importance of both the magnitude and range of specific binding interactions for adhesion protein function, and the dependence of intermembrane potentials on the complicated architectures of these molecules. Our unique ability to measure forces between adhesion proteins as a function of the intersurface distance resulted in the discovery of multidomain, modular interactions between cell adhesion proteins. They further reveal that the molecular mechanisms of protein-mediated adhesion, in general, are much richer than originally thought.

ABBREVIATIONS

APC	antigen-presenting cell
EC1-5	cadherin extracellular (EC) domains one through five
EC1	cadherin extracellular domain one
Ig	immunoglobulin
FN III	fibronectin type III
MHC	major histocompatibility complex
NCAM	neural cell adhesion molecule
PSA	polysialic acid
rCD2	CD2 purified from rat tissue
hCD2	CD2 purified from human tissue
SFA	surface force apparatus
TCR	Tcell receptor

REFERENCES

[1] Yap, A. S., Brieher, W. M., and Gumbiner, B. M., *Annu. Rev. Cell. Dev. Biol.* **13**, 119–146 (1997).

[2] Marshall, B. T., Long, M., Piper, J. W., Yago, T., McEver, R. P., and Zhu, C., *Nature* **423**, 190–193 (2003).

[3] Dembo, M., Torney, D. C., Saxman, K., and Hammer, D., *Proc. R. Soc. Lond. B.* **234**, 55–83 (1988).
[4] Bell, G. I., Dembo, M., and Bongrand, P., *Biophys. J.* **45**, 1051–1064 (1984).
[5] Bell, G. I., *Science* **200**, 618–627 (1978).
[6] Torney, D. C., Dembo, M., Bell, G. I., *Biophys. J.* **49**, 501–507 (1986).
[7] Soto, G. and Hultgren, S. J., *J. Bacteriol.* **181**, 1059–1071 (1999).
[8] Albersdorfer, A., Feder, T., and Sackmann, E., *Biophys. J.* **73**, 245–257 (1997).
[9] Lauffenburger, D. A. and Linderman, J. J., Receptors: Models for Binding, Trafficking, and Signalling, (Oxford University Press, NY, 1993).
[10] Chothia, C. and Jones, E. Y., *Ann. Rev. Biochem.* **66**, 823–862 (1997).
[11] Walsh, F. and Doherty, P., *Ann. Rev. Cell. Biol.* **13**, 425–456 (1997).
[12] Zhu, B., Davies, E. A., van der Merwe, A., and Leckband, D., *Biochemistry* **42**, 12163–12170 (2002).
[13] Zhu, B., Chappuis-Flament, S., Wong, E., Jensen, I., Gumbiner, B. M., and Leckband, D. E., *Biophys. J.* **41**, 12163–12170 (2003).
[14] Sivasankar, S., Gumbiner, B. M., and Leckband, D., *Biophys. J.* **80**, 1758–1768 (2001).
[15] Sivasankar, S., Brieher, W., Lavrik, N., Gumbiner, B., and Leckband, D., *Proc. Natl. Acad. Sci. USA* **96**, 11820–11824 (1999).
[16] Florin, E.-L., Moy, V. T., and Gaub, H. E., *Science* **264**, 415–417 (1994).
[17] Rief, M., Gautel, M., Oesterhelt, F., Fernandez, J. M., and Gaub, H. E., *Science* **276**, 1109–1112 (1999).
[18] Leckband, D. and Israelachvili, J. N., *Quart. Rev. Biophys.* **34**, 105–267 (2001).
[19] Israelachvili, J., *Surface Science Reports* **14**, 110–159 (1992).
[20] Israelachvili, J., *J. Coll. Int. Sci.* **44**, 259–272 (1973).
[21] Israelachvili, J. and McGuiggan, P., *J. Mater. Res.* **5**, 2223–2231 (1990).
[22] Marra, J. and Israelachvili, J., *Biochemistry* **24**, 4608–4618 (1985).
[23] Israelachvili, J., Intermolecular and Surface Forces, (Academic Press, New York, 1991).
[24] Johnson, K. L., Kendall, K., and Roberts, A. D., *Proc. R. Soc. Lond. A.* **324**, 301–313 (1971).
[25] Vijayendran, R., Hammer, D., and Leckband, D., *J. Chem. Phys.* **108**, 1162–1169 (1998).
[26] Yeung, C., Purves, T., Kloss, A. A., Kuhl, T. L., Sligar, S., and Leckband, D., *Langmuir* **15**, 6829–6836 (1999).
[27] Leckband, D. E., Kuhl, T. L., Wang, H. K., Müller, W., and Ringsdorf, H., *Biochemistry* **34**, 11467–11478 (1995).
[28] Bromley, S. K., Burack, W. R., Johnson, K. G., Somersalo, K., Sims, T. N., Sumen, C., Davis, M. M., Shaw, A. S., Allen, P. M., and Dustin, M. L., *Annu. Rev. Immunol.* **19**, 375–396 (2001).
[29] Grakoui, A., Bromley, S. K., Sumen, C., Davis, M. M., Shaw, A. S., Allen, P. M., and Dustin, M. L., *Science* **285**, 221–226 (1999).
[30] Alberts, B., Bray, D., Lewis, J., Raff, M., Roberts, K., and Watson, J. D., The Molecular Biology of the Cell, (Garland, NY, 1983).
[31] Qi, S. Y., Groves, J. T., and Chakraborty, A. K., *Proc. Natl. Acad. Sci.* **98**, 6548–6553 (2001).
[32] Davis, S. J. and van der Merwe, P. A., *Science* **273**, 1241–1242 (1996).
[33] Davis, S. J. and van der Merwe, P. A., *Immunol. Today* **17**, 177–187 (1996).
[34] van der Merwe, P. A., Brown, M. H., Davis, S. J., and Barclay, N. A., *EMBO J.* **12**, 4945–4954 (1993).

[35] Bodian, D. L., Jones, E. Y., Stuart, D. I., and Davis, S. J., *Structure* **2**, 755–766 (1994).
[36] Driscoll, P. C., Cyster, J. G., Campbell, I. D., and Williams, A. F., *Nature* **353**, 762–765 (1991).
[37] Jones, E. Y., Davis, S. J., Williams, A. F., Harlos, K., Stuart, D. I., *Nature* **360**, 232–239 (1992).
[38] McAlister, M. S. B., Mott, H. R., van der Merwe, P. A., Campbell, I. D., Davis, S. J., and Driscoll, P. C., *Biochemistry* **35**, 5982–5991 (1996).
[39] van der Merwe, P. A., Barclay, A. N., Mason, D. W., Davies, E. A., Morgan, B. P., Tone, M. Krishnam, A. K. C., Ianelli, C., and Davis, S. J., *Biochemistry* **33**, 10149–10160 (1994).
[40] Davis, S. J., Davies, E. A., Tucknott, M. G., Jones, E. Y., and van der Merwe, A., *Proc. Natl. Acad. Sci. USA* **95**, 5490–5494 (1998).
[41] Takeichi, M., *Curr. Opin. Cell Biol.* **7**, 619–627 (1995).
[42] Takeichi, M., *Science* **251**, 1451–1455 (1991).
[43] Steinberg, M. S. and Takeichi, M., *Proc. Natl. Acad. Sci. USA* **91**, 206–209 (1994).
[44] Steinberg, M. S. and McNutt, P. M., *Curr. Opin. Cell. Biol.* **11**, 554–560 (1999).
[45] Meyer, R. L., *Neuropsychologia* **36**, 957–980 (1998).
[46] Shapiro, L., Fannon, A. M., Kwong, P. D., Thompson, A., Lehmann, M. G., Grübel, G., Legrand, J.-F., Als-Nielsen, J., Colman, D. R., and Hendrickson, W. A., *Nature* **374**, 327–337 (1995).
[47] Nose, A., Tsuji, K., and Takeichi, M., *Cell* **61**, 147–155 (1990).
[48] Koch, A., Bozic, D., Pertz, O., and Engel, J., *Curr. Opin. Struct. Biol.* **9**, 275–281 (1999).
[49] Chappuis-Flament, S., Wong, E., Hicks, L. D., Kay, C. M., and Gumbiner, B. M., *J. Cell Biol.* **154**, 231–243 (2001).
[50] Renaud-Young, M. and Gallin, W. J., *J. Biol. Chem.* **277**, 39609–39616 (2002).
[51] Martel, L., Johnson, C., Boutet, S., Al-Kurdi, R., Konovalov, O., Robinson, I., Leckband, D., and Legrand, J-F., *J. Phys. IV* **12(PR6)**, 365–377 (2002).
[52] Baumgartner, W., Hinterdorfer, P., Ness, W., Rash, A., Vestweber, D., Schindler, H., and Drenckhahn, D., *Proc. Natl. Acad. Sci.* **97**, 4005–4010 (2000).
[53] Boggon, T., Murray, J., Chappuis-Flament, S., Wong, E., Gumbiner, B. M., Shapiro, L., *Science* **296**, 1308–1313 (2002).
[54] Tamura, K., Shan, W.-S., Hendrickson, W. A., Colman, D. R., and Shapiro, L., *Neuron* **20**, 1153–1163 (1998).
[55] Nagar, B., Overduin, M., Ikura, M., and Rini, J. M., *Nature* **380**, 360–364 (1995).
[56] Becker, J. W., Erickson, H. P., Hoffmann, S., Cunningham, B. A., and Edelman, G. M., *Proc. Natl. Acad. Sci. USA* **86**, 1088–1092 (1989).
[57] Hall, A. K. and Rutishauser, U., *J. Cell. Biol.*, **104**, 1579–1586 (1987).
[58] Cunningham, B. A., Hemperly, J. J., Murray, B. A., Prediger, E. A., Brackenbury, R., and Edelman, G. M., *Science* **236**, 799–806 (1987).
[59] Rao, Y., Wu, X-F., Gariepy, J., Rutishauser, U., and Siu, C.-H., *J. Cell Biol.* **118**, 937–949 (1992).
[60] Atkins, A. R., Chung, J., Songpon, D., Little, E., Edelman, G. M., Wright, P. E., Cunningham, B. A., Dyson, H. J., *J. Mol. Biol.* **311**, 161–172 (2001).
[61] Kiselyov, V., Berezin, V., Maar, T. E., Soroka, V., Edvardsen, K., Schousboe, A., Bock, E., *J. Biol. Chem.* **93**, 4071–4075 (1997).
[62] Jenson, P., Soroka, V., Thompson, N. K., Ralets, I., Berezin, V., Bock, E., and Poulsen, F. M., *Nature Struct. Biol.* **6**, 486–493 (1999).
[63] Kasper, C., Rasmussen, H., Kastrup, J. S., Ikemizu, S., Jones, R. Y., Berezin, V., Bock, E., and Larsen, I. K., *Nature Struct. Biol.* **7**, 389–393 (2000).

[64] Soroka, V., Kiryushko, D., Novitskaya, V., Ronn, C. B., Poulson, F. M., Holm, A., Bock, E., and Berezin, V., *J. Biol. Chem.* **277**, 24676–24683 (2002).
[65] Soroka, V., Kolkova, K., Kastrup, J. S., Diederichs, K., Breed, J., Kiselyov, V. V., Poulsen, F. M., Poulsen, F. M., Larsen, I. K., Welte, W., Berezin, V., Bock, E., and Kasper, C., *Structure* **10**, 1291–1301 (2003).
[66] Johnson, C. P., Fujimoto, I., Perrin-Tricaud, C., Rutishauser, U., and Leckband, D., *Proc. Natl. Acad. Sci. USA* **101**, 6963–6968 (2004).
[67] Rutishauser, U., *Curr. Opin. Cell Biol.* **8**, 679–684 (1996).
[68] Acheson, A., Sunshine, J. L., and Rutishauser, U., *J. Cell Biol.* **114**, 143–153 (1991).
[69] Nelson, R. W., Bates, P. A., and Rutishauser, U., *J. Biol. Chem.* **270**, 17171–17179 (1995).
[70] Rutishauser, U., Grumet, M., *et al., J. Cell. Biol.* **97**, 145–152 (1983).
[71] Tanaka, F., Otake, Y., Nakagawa, T., Kawano, Y., Miyahara, R., Li, M., Yanagihara, K., Nakayama, J., Fujimoto, I., Ikenaka, K., and Wada, H., *Cancer Res.* **60**, 3072–3080 (2000).
[72] Landmesser, L., Dahm, L., *et al., Neuron* **4**, 655–667 (1990).
[73] Yang, P., Yin, X., and Rutishauser, U., *J. Cell Biol.* **116**, 1487–1496 (1992).
[74] Fujimoto, I., Bruses, J. L., Rutishauser, U., *J. Biol. Chem.* **276**, 31745–31751 (2001).
[75] Hunter, R., Foundations of Colloid Science, Volume 1, (Oxford University Press, Oxford, 1989).
[76] Johnson, C. P., Fujimoto, I., Rutishauser, U., and Leckband, D., *unpublished observations*, (2004).
[77] Yang, P., Major, D., and Rutishauser, U., *J. Biol. Chem.* **269**, 23039–23044 (1994).
[78] Grumet, M., *Cell Tissue Res.* **290**, 423–428 (1997).